THE JOURNAL OF BIOLOGICAL CHEMISTRY
Vol. 280, No. 15, Issue of April 15, pp. 14819–14828, 2005

*Printed in U.S.A.*

# BmP09, a "Long Chain" Scorpion Peptide Blocker of BK Channels*

Received for publication, November 10, 2004, and in revised form, January 18, 2005
Published, JBC Papers in Press, January 28, 2005, DOI 10.1074/jbc.M412735200

**Jing Yao‡§, Xiang Chen§¶, Hui Li‡, Yang Zhou‖**, Lijun Yao‖**, Gong Wu¶, Xiaoke Chen‖**, Naixia Zhang¶, Zhuan Zhou‖**, Tao Xu‡ ‡‡, Houming Wu¶§§, and Jiuping Ding‡¶¶**

*From the ‡Institute of Biochemistry and Biophysics, College of Life Science and Technology, Huazhong University of Science and Technology, Wuhan, Hubei 430074, ¶State Key Laboratory of Bio-organic and Natural Products Chemistry, Shanghai Institute of Organic Chemistry, Chinese Academy of Sciences, Shanghai 200032, ‖Institute of Molecular Medicine, Peking University, Beijing 100031, **Institute of Neuroscience, SIBS, Chinese Academy of Sciences, Shanghai 200031, and ‡‡National Laboratory of Biomacromolecules, Institute of Biophysics, Chinese Academy of Sciences, Beijing 100101, China*

**A novel "long chain" toxin BmP09 has been purified and characterized from the venom of the Chinese scorpion *Buthus martensi* Karsch. The toxin BmP09 is composed of 66 amino acid residues, including eight cysteines, with a mass of 7721.0 Da. Compared with the *B. martensi* Karsch AS-1 as a $Na^+$ channel blocker (7704.8 Da), the BmP09 has an exclusive difference in sequence by an oxidative modification at the C terminus. The sulfoxide Met-66 at the C terminus brought the peptide a dramatic switch from a $Na^+$ channel blocker to a $K^+$ channel blocker. Upon probing the targets of the toxin BmP09 on the isolated mouse adrenal medulla chromaffin cells, where a variety of ion channels coexists, we found that the toxin BmP09 specifically blocked large conductance $Ca^{2+}$- and voltage-dependent $K^+$ channels (BK) but not $Na^+$ channels at a range of 100 nM concentration. This was further confirmed by blocking directly the BK channels encoded with mSlo1 $\alpha$-subunits in *Xenopus* oocytes. The half-maximum concentration $EC_{50}$ of BmP09 was 27 nM, and the Hill coefficient was 1.8. In outside-out patches, the 100 nM BmP09 reduced ~70% currents of BK channels without affecting the single-channel conductance. In comparison with the "short chain" scorpion peptide toxins such as Charybdotoxin, the toxin BmP09 behaves much better in specificity and reversibility, and thus it will be a more efficient tool for studying BK channels. A three-dimensional simulation between a BmP09 toxin and an mSlo channel shows that the Lys-41 in BmP09 lies at the center of the interface and plugs into the entrance of the channel pore. The stable binding between the toxin BmP09 and the BK channel is favored by aromatic $\pi$-$\pi$ interactions around the center.**

Large conductance $Ca^{2+}$- and voltage-dependent potassium (MaxiK, BK) channels are thought to play a primary role in a link between the membrane potential and the cellular calcium homeostasis. BK channels are very abundant in many tissues from pancreas to smooth muscle to brain (1). Natural toxins are among the most potent and important tools for studying the functions and structure of ion channels. Various species such as the sea anemone, snakes, cone snails, spiders, and scorpions possess ion channel toxins in their venom (2). $\kappa$ conotoxin BtX ($\kappa$-BtX) coming from the venom of a worm-hunting cone snail enhances the currents of BK (3). Another toxin from the medicine herb dehydrosoyasaponin-1 (DHS-1) also increases the BK currents when the $\alpha$-subunit coexists with its $\beta$-subunit (4). Scorpion venoms are rich sources of fascinating neurotoxins, which bond with high affinity and specificity to various ion channels and thus widely serve as useful tools in probing the protein mapping of ion channels and clarifying the molecular mechanism involved in the signal transmission and channel gating. Some of the peptidyl scorpion toxins such as Charybdotoxin (ChTX),[1] Iberiotoxin, and Slotoxin also block the BK currents encoded by both the Slo1 $\alpha$-subunits and the $\beta$-subunits but with a higher $EC_{50}$ (5, 6). Those toxins have in common very poor reversibility, which makes it difficult to study the functions of BK currents, especially in current clamp experiments, even though this property is often used to identify the existence of $\beta$-subunits (7–9). Recently, Xu *et al.* (10) found another scorpion toxin BmBKTx1 that blocks pSlo (82 nM) and dSlo (194 nM),but not hSlo. According to its specific characteristics, BmBKTx1 can be used to identify different subunits involved in BK channels. So far more than 120 peptide modulators of ion channels have been isolated from scorpion venoms. Most of the scorpion toxins blocking $K^+$ channels (KTx) are short peptides (22–43 amino acids residues) with a well conserved three-dimensional structure stabilized by three or four disulfide bridges (11).

The Chinese scorpion *Buthus martensi* Karsch (BmK) has been used as traditional medicine in China for more than 1000 years, especially for treatments in neural diseases such as apoplexy, hemiplegia, and facial paralysis (12). Indeed, over the past decade, more than 70 different peptides, toxins, or homologues have been isolated. Among them, 14 short chain peptides are associated with the $K^+$ channel toxin family; 51 long chain peptides are related to the $Na^+$ channel toxin family, and only one long chain peptide is identified as a blocker of voltage-dependent $K^+$ channels ($K_V$) (2).

* This work was supported by National Science Foundation of China Grants 20132030, 30025023, 30470445, 3000062, 30130230, 30328013, and 30330210, the Major State Basic Research Program of People's Republic of China Grants 2004CB720000, 2001CCA04100, and G2000077800, the Li Foundation and the Sinogerman Scientific Center, and Chinese Academy of Sciences Grant KGCX2-SW-213-05. The costs of publication of this article were defrayed in part by the payment of page charges. This article must therefore be hereby marked "*advertisement*" in accordance with 18 U.S.C. Section 1734 solely to indicate this fact.

§ Both authors contributed equally to this work.

§§ To whom correspondence may be addressed. E-mail: hmwu@mail.sioc.ac.cn.

¶¶ To whom correspondence may be addressed. Tel.: 86-27-8779-2024; Fax: 86-27-8779-2024; E-mail: jpding@mail.hust.edu.cn.

[1] The abbreviations used are: ChTX, Charybdotoxin; MACCs, mouse adrenal medulla chromaffin cells; MS, mass spectrometry; ESI-MS, electrospray ionization-mass spectrometry; Tricine, *N*-[2-hydroxy-1,1-bis(hydroxymethyl)ethyl]glycine; TEA, tetraethylammonium; HPLC, high pressure liquid chromatography; BmK, *B. martensi* Karsch.

In our previous paper (13), a systematic isolation has been achieved, and 11 short chain peptides have been characterized from the venom of the Chinese scorpion BmK. Solution structures of some short chain scorpion toxins (less than 40 amino acid residues long) have been described previously (14–16). Here we report on the purification, characterization, and sequence determination of a novel BK potassium channel blocker BmP09, which is composed of a long chain (66 amino acid residues long) with four disulfide bridges. By assaying the effects of BmP09 on voltage-gated channels in MACCs and on BK channels (mSlo) expressed in *Xenopus* oocytes, we found that BmP09 was a better specific blocker of BK channels encoded by mSlo $\alpha$-subunits with perfect reversibility; in other words, it only took less than 5 s for a full recovery. Compared with the Charybdotoxin (ChTX), the superior selectivity and reversibility makes BmP09 a better tool for the structural and functional studies on BK channels.

## EXPERIMENTAL PROCEDURES

### *Purification and Chemical Characterization of Toxin BmP09*

Crude venom was collected by electrical stimulation of the telson of scorpion BmK bred in captivity in Henan Province, China. The peptide was purified as described previously (13). Lyophilized crude venom was dissolved in $NH_4HCO_3$ buffer (50 mM, pH 8.5) and centrifuged at $4000 \times g$ for 15 min. The supernatant was loaded onto a Sephadex G-50 column (2.5 × 150 cm, Amersham Biosciences), which was equilibrated and eluted with the same buffer (Fig. 1*A*). Fraction III from the Sephadex G-50 column was loaded onto a Mono S cation exchange column (HR 5/5, Amersham Biosciences), eluted with a step gradient of solution A to solution B at pH 5.0 (Fig. 1*B*). Solution A contained NaAc (20 mM), and solution B contained NaAc (20 mM) and NaCl (1 M). It was followed by similar separation on another Sephadex G-50 column (Fig. 1*C*). The final purification of BmP09 (G3512) was performed by using a reverse-phase HPLC column ($C_{18}$ column, 4.6 × 250 mm, 5 $\mu$m bead size, Alltech) eluted with a linear gradient from solution C to 50% solution D in solution C at a flow of 1 ml/min. Solution C contained $CH_3CN$ (10%) and trifluoroacetic acid (0.1%) in $H_2O$, and solution D contained $H_2O$ (20%) and trifluoroacetic acid (0.1%) in $CH_3CN$ (Fig. 1*D*).

The molecular weight of BmP09 was measured using a LCMS-2010A ESI-MS instrument (Shimadazu, Japan). Amino acid analysis was performed on a Beckman 6300 apparatus (Beckman) after hydrolysis of the sample in HCl (6 M) under vacuum at 110 °C for 18 h. The N-terminal sequence of BmP09 was achieved by Edman degradation using a Beckman LF3200 protein-peptide sequencer.

### *Primary Sequence Determination of BmP09*

Because of the existence of disulfide bonds in the sequence, the sample of BmP09 was subjected to dithiothreitol reduction and iodoacetamide derivatization before MS analysis. Peptide BmP09 was reduced with a 250-fold molar excess of dithiothreitol in 0.25 M Tris-HCl buffer (pH 8.5) containing 6 M guanidine HCl and 4 mM EDTA. Reduction was carried out in the dark under nitrogen at 37 °C for 1 h. Free thiols were alkylated by addition of a 500-fold molar excess of iodoacetamide held at room temperature for 30 min in the dark. The sample was load onto a 10% Tris-Tricine gel for SDS-PAGE to remove reagents. Peptide mapping study was performed on *S*-alkylated BmP09 as the L-1-tosylamido-2-phenylethyl chloromethyl ketone-treated trypsin took place *in situ* in the gel after electrophoresis. AutoMS-Fit automation software was used to analyze the masses of peptide fragments obtained by digestion.

A sample of BmP09 (100 $\mu$l, 50 ng/$\mu$l) was digested with carboxypeptidase P and Y (Sigma, 0.2 ng/$\mu$l, enzyme/substrate ratio was 1:500, w/w) in aqueous solution at 25 °C. Every 6.0-$\mu$l digested sample was taken out at 20, 40, and 60 s, 2, 5, 10, 15, 20, 30, and 60 min, and 2 and 4 h after the onset of incubation, and each aliquot was acidified with 1% trifluoroacetic acid and lyophilized immediately. Each lyophilized sample was mixed at the ratio of 1:1 with a 4 mg/ml solution of $\alpha$-cyano-4-hydroxycinnamic acid ($CH_3OH$:$H_2O$, 0.1% trifluoroacetic acid) and performed by a matrix-assisted laser desorption ionization time-of-flight MS spectrum using a Voyager-DE STR (Applied Biosystems) operated in the reflection mode with time lag focusing.

### *Electrophysiology and Solutions*

*Chromaffin Cell Preparation*—Based on several early studies (17, 18), MACCs were isolated and maintained as described previously. To compare the effects of BmP09 and BmK AS-1 in the patch clamp experiments, we used rat adrenal chromaffin cells (3, 16, 19). Dispersion of chromaffin cells was typically done on adrenal medullas from two or three Wistar mice (20–30 g) ~1 month of age. Cells were cultured with Dulbecco's modified Eagle's medium in a standard $CO_2$ incubator at 37 °C, and currents were recorded 1–5 days after plating.

*Mutagenesis*—Point mutations of mSlo, F266L and F266A, were produced by using QuikChange protocol (Stratagene). In brief, PCRs were performed by using the wild-type mSlo as a template and a pair of complementary mutagenesis primers (F266L,5′-CAGGGGACCCATGGGAAAATCTTCAAAACAACCAGGCACTTAC-3′ and 5′-GTAAGTGCCTGGTTGTTTTGAAGATTTTCCCATGGGTCCCCTG-3′; F266A, 5′-CAGGGGACCCATGGGAAAATGCTCAAAACAACCAGGCACTTACG-3′ and 5′-CGTAAGTGCCTGGTTGTTTTGAGCATTTTCCCATGGGTCCCCTG-3′). The PCR mixture was then cut with the enzyme DpnI to digest the template wild-type mSlo. After DpnI digestion, the PCR product was transformed into competent bacterial cells to amplify the mutant plasmid of mSlo. Both mutant constructs were verified by sequencing.

*Expression in Xenopus Oocytes*—Methods of expression in stage V–VI *Xenopus* oocytes were as described previously (7). Oocytes were defolliculated by treatment with 2 mg/ml collagenase I (Sigma) in zero calcium ND-96 solution. Between 2 and 24 h after defolliculation, 1–2 ng (mSlo) cRNA (a gift of Dr. Christopher Lingle, Washington University, St. Louis, MO) were injected into *Xenopus* oocytes using a Drummond Nanoject II (Drummond Scientific Co.). After injection, oocytes were then incubated in ND-96 solution at 18 °C. Currents were recorded 2–7 days after RNA injection. ND-96 solution (pH 7.5) containing the following concentrations (in mM), 96 NaCl, 2 KCl, 1.8 $CaCl_2$, 1 $MgCl_2$, 2.5 sodium pyruvate, and 10 $H^+$-HEPES, were supplemented with 100 IU/ml penicillin and 100 $\mu$g/ml streptomycin (only for incubation).

*Solutions*—For MACCs, the normal extracellular solution contained the following (in mM): 150 NaCl, 5.4 KCl, 1.8 $CaCl_2$, 2 $MgCl_2$, and 10 $H^+$-HEPES (pH 7.4) titrated with NaOH. For whole-cell recording, the standard pipette solution contained the following (in mM): 130 potassium glutamine, 30 KCl, 0.1 EGTA, 10 $H^+$-HEPES, 0.05 GTP, and 2 MgATP (pH 7.4). The "high tetraethylammonium chloride (TEA)" solution was the same as the standard bath solution except that the 20 mM NaCl was replaced by 20 mM TEA. The "high $Cs^+$" solution contained the following (in mM): 130 cesium glutamine, 30 CsCl, 0.1 EGTA, 10 $H^+$-HEPES, 0.05 GTP, and 2 MgATP (pH 7.4).

To record $Na^+$ currents, the high TEA solution was used as a bath solution, and pipettes were backfilled with high $Cs^+$ solution. For $Ca^{2+}$ current recording solutions, the bath solution contained the following (in mM): 160 TEA, 5 $BaCl_2$, 10 $H^+$-HEPES, and 0.1 EGTA, with pH adjusted to 7.4 with tetraethylammonium hydroxide, and the pipette solution was the high $Cs^+$ solution. For oocytes, during recordings, oocytes were bathed in the solution containing the following (in mM): 160 $MeSO_3K$, 10 $H^+$-HEPES, and 2 $MgCl_2$, adjusted to pH 7.0 with $MeSO_3H$. Pipettes were filled with a solution containing the following (in mM): 160 $MeSO_3K$, 10 $H^+$-HEPES, and 5 *N*-hydroxyethylenediaminetriacetic acid (HEDTA) with added $Ca^{2+}$ to make 10 $\mu$M free $Ca^{2+}$, as defined by the EGTAETC program (E. McCleskey, Vollum Institute, Portland, OR), with the pH adjusted to 7.0. All of the chemicals were obtained from Sigma.

*Patch Clamp Recording from Single Cells*—Patch pipettes pulled from borosilicate glass capillaries had resistances of 2–6 megohms when filled with internal solution. An outside-out patch was obtained by excising the patch from a cell in the whole-cell configuration. Experiments were performed and recorded using an EPC-9 patch clamp amplifier and PULSE software (HEKA Electronics, Germany). Currents were typically digitized at 20 kHz. Macroscopic records were filtered at 2.9 kHz during digitization. Single-channel records were filtered at 10 kHz.

During recording, drugs and control/wash solutions were puffed locally onto the cell via a puffer pipette containing seven solution channels. The tip (300 $\mu$m diameter) of the puffer pipette was located about 120 $\mu$m from the cell. As determined by the conductance tests, the solution around a cell under study was fully controlled by the application solution with a flow rate of 100 $\mu$l/min or greater. All pharmacological experiments met this criterion. All these experiments were done at room temperature (22–25 °C).

### *Data Analysis*

Data were analyzed with IGOR (Wavemetrics, Lake Oswego, OR), Clampfit (Axon Instruments, Inc.), SigmaPlot (SPSS Inc.), and QUB

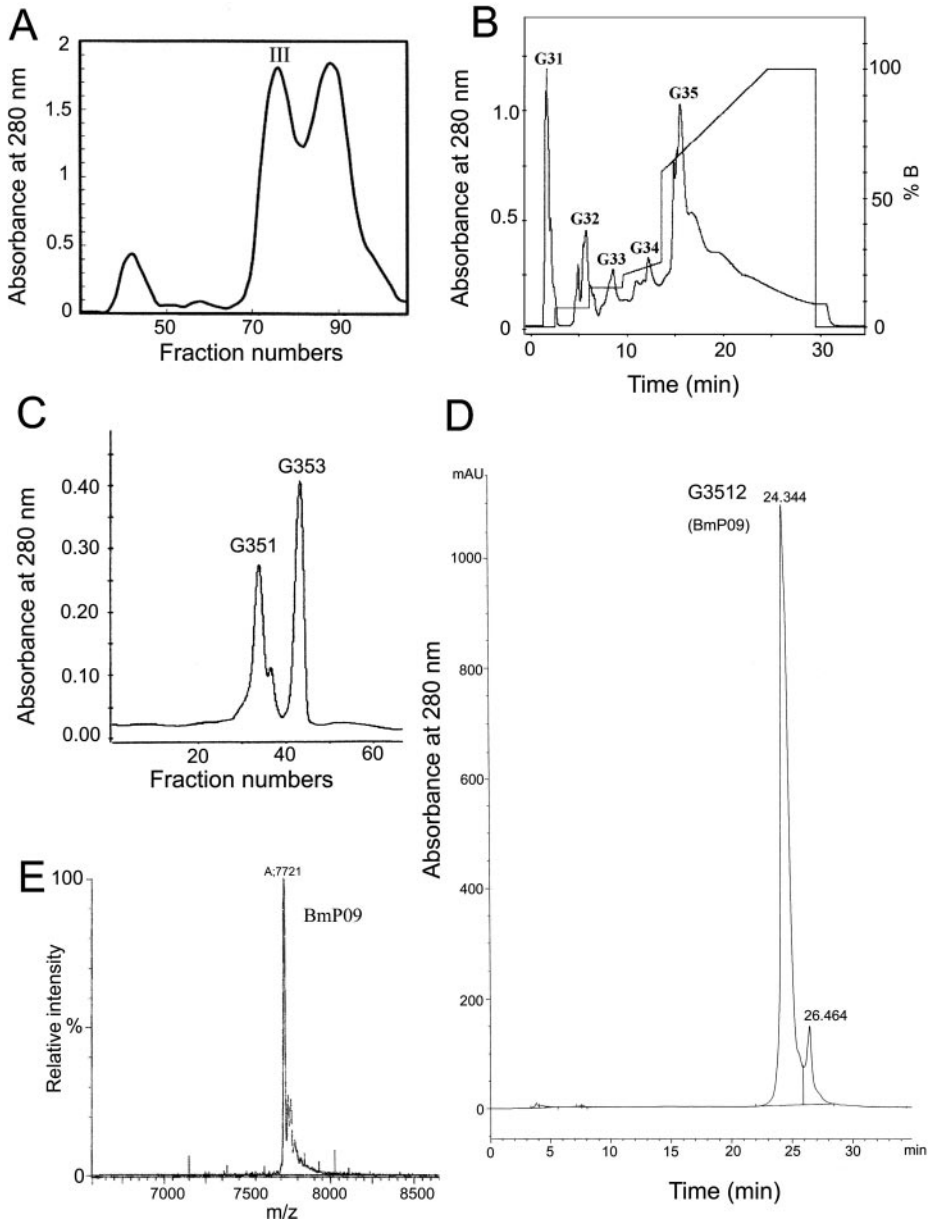


FIG. 1. **Isolation and purification of BmP09.** *A*, Sephadex G-50 column chromatography of the crude venom of *B. martensi* Karsch. *B*, fast protein liquid chromatography separation of the fraction III from procedure *A* on Mono S cation exchange column. *C*, Sephadex G-50 column chromatography from the fraction G35 of procedure *B*. *D*, RP-HPLC purification of the fraction G351 of the procedure *C* on a C18 column. *E*, ESI-MS spectrum of BmP09.

(State University of New York, Buffalo) software. Unless stated otherwise, the data are presented as means ± S.E.; significance was tested by Student's *t* test, and differences in the mean values were considered significant at a probability of ≤0.05.

Dose-response curve for the percent block of BK currents was drawn according to the Hill equation $I = I_m/(1 + ([toxin]/EC_{50})^n)$, where $I_m$ is maximum blocking percentage of BK currents, and [toxin] is the concentration of BmP09. $EC_{50}$ and $n$ denote the toxin concentration of half-maximal effect and the Hill coefficient, respectively.

### *Homology Modeling and Docking Experiment*

The model of BK channel (20) was generated by homology modeling on the basis of the crystal structure of the bacterial KcsA channel (Protein Data Bank code 1BL8) (21), using the software SYBYL6.3 (Tripos Associates). The sequence alignment between KcsA and BK channel was obtained using the same criteria as those described by Gao and Garcia (22). The homology model of BK channel was further subjected to Powell minimization (2000 steps) using Kollman force field.

The models of toxin BmP09 and BmK AS-1 (23) were generated by homology modeling on the basis of the crystal structure of the toxin neurotoxin 2 (Protein Data Bank code 1JZB) (24). The sequence alignment between them is described in Fig. 3. The homology models of toxins BmP09 and BmK AS-1 were further subjected to energy minimization and dynamic simulation.

The surface electrostatic distribution analysis indicated that BmP09 preferred association with the entryway of the $K^+$ channel by using the positively charged patch with the side chain of Lys-41 in the center. The program "O" (version 8.0.6) (25) was used for the docking experiment. BmP09 was docked manually into the outer entryway of the BK channel model along with the dipole direction. As expected, the mouth of the $K^+$ channel bears a large negative charge, whereas the surface of the toxin BmP09 has a positive charge. The electrostatic potential between the toxin BmP09 and the $K^+$ channel attracted the positively charged toxin to the entryway of the channel. In order to obtain favorable toxin-channel clusters, the toxin molecule was allowed to rotate during the docking process. The most stable cluster with the best fit between the toxin and the $K^+$ channel was used to analyze the contacts between the BmP09 and the BK channel.

The BmP09-BK channel cluster docked most favorably was further subjected to energy minimization for 2000 steps to achieve the gradient tolerance 0.05 kcal/(mol Å) using the Powell algorithm and the Kollman force field in the software SYBYL6.3. Molecular dynamics simulation using the Powell algorithm was then carried out for the complex for 100 fs at 300 K. Kollman force field constraints were applied on the backbones of the channel in the region comprising residues His-254 to Val-0278, whereas the remaining part of the channel was kept fixed during the simulation. The structure of the peptide was completely unconstrained. A cut-off distance of 8 Å was used for nonbounded interactions. An integration time step of 0.1 fs was used, and coordinate sets of the trajectory were saved every 2 fs. Every structure obtained

from the coordinate sets over the 100 fs of simulation was performed with 500 steps of minimization. Finally, the average structure was energy-minimized with 1000 steps of Powell minimization.

## RESULTS

*Purification of BmP09*—The crude venom was initially separated into four fractions (I–IV) by gel filtration chromatography on a Sephadex G-50 column (Fig. 1*A*). Separation of the fraction III on a Mono S cation exchange column gave five fractions (Fig. 1*B*). Among the five fractions, fraction 5 was further separated on another Sephadex G-50 column, and two sub-fractions 351 and 353 were obtained (Fig. 1*C*). A pure peptide was obtained after the separation of fraction 351 on a reverse-phase HPLC column (Fig. 1*D*).

*Primary Sequence of BmP09*—The molecular weight of BmP09 was 7721 Da, as determined by ESI-MS (Fig. 1*E*). The results of the amino acid analysis (Table I), the N-terminal 14-residue sequence analysis (DNGYLLNKYTGCKI), and peptide mapping studies (Fig. 2) are consistent with those calculated from the mature peptide BmK AS-1 derived from cDNA (GenBank™ accession number AF079061). The difference in molecular weight between the ESI-MS data (7721 Da) and calculated value (7704.8 Da) according to the sequence of BmK AS-1 could be attributed to the oxidation of the C-terminal Met residue (26). The oxidative modification could be validated by the MS analysis of the carboxypeptidase-digested products. Actually, a principal ion with the MS value of 7575 Da was observed under the molecular ion in the MS spectrum of the carboxypeptidase-digested products. The mass difference (147 Da) is well accounted for a Met residue with a sulfoxide group. Therefore, the sequence of BmP09 is the same to that of BmK AS-1, and only differs at the C terminus by an oxidative modification (see Fig. 3).

TABLE I
*The amino acid compositions of BmP09*

| Amino acid | No. residues |
|---|---|
| Asx | 8.77 (9) |
| Thr | 1.87 (2) |
| Ser | 2.06 (3) |
| Glx | 5.57 (5) |
| Gly | 5.93 (6) |
| Ala | 3.06 (3) |
| Val | 1.56 (1) |
| Met | 0.85 (1) |
| Ile | 1.98 (2) |
| Leu | 5.02 (5) |
| Tyr | 5.37 (7) |
| Phe | 1.35 (1) |
| Arg | 2.04 (2) |
| Lys | 6.57 (7) |
| Pro | 1 |
| Trp | 3 |
| Cys-Cys | 3.17 (4) |
| $M_h$ (calculated) | 7704.81 |
| $M_h$ (experimental) | 7721 |

*Effects of BmP09 on Voltage-gated Channels in Chromaffin Cells*—MACCs are excitable cells and express variety of voltage-gated channels such as voltage-gated $Na^+$, $K^+$, and $Ca^{2+}$ channels. They are widely used as a neuronal model for studying the features of channel behaviors and searching the targets of toxins (27–31). To study whether the BmP09 affects voltage-gated ion channels, we started to screen for its effects on the MACCs. As shown in Fig. 4*A*, whole-cell currents were elicited by 60-ms voltage ramps from −90 to +100 mV within the normal extracellular solution in the presence and absence of 100 nM BmP09. With the augmentation of the membrane potential by the voltage ramp, inward currents of $Na^+$ and $Ca^{2+}$ channels first emerged at ~0 mV, and the outward currents of voltage-gated $K^+$ channels, including both the $K_V$ and the $K_{Ca}$ channels, started to increase gradually (28, 31). In Fig. 4*A*, the *dark trace* shows a 67% reduction of outward maximum currents, by the application of 100 nM BmP09, with a slight increase in inward currents. The reduction of outward currents may result in the slight increase of inward currents. In addition, after removal of BmP09, the current trace indicated in Fig. 4*A* is almost back to the control level, which hints that the blocking behavior of BmP09 is reversible.

Voltage-gated sodium channels play a critical role in the repeated firing of action potentials and propagation in excitable cells (2). Most of the long chain peptides have been proved to be the blockers of $Na^+$ channels such as BmK AS-1 (32). However, the traces in Fig. 4*B*, activated by voltage steps to 0 mV after a prepulse to −90 mV to remove inactivation, are overlaid to emphasize that there is no inhibition on $Na^+$ channels before, during, and after the application of the toxin 100 nM BmP09. In contrast, BmK AS-1 has an inhibitive effect on the $Na^+$ channel in chromaffin cells (32) but no effect on the $K^+$ currents ($n = 5$, data not shown). In chromaffin cells, most types of calcium

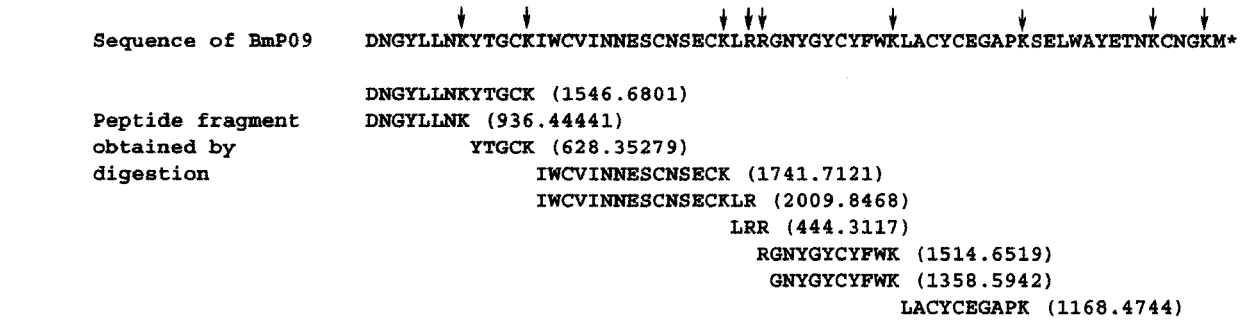


FIG. 2. **Peptide mapping for the fragments.** Peptide mapping comes from L-1-tosylamido-2-phenylethyl chloromethyl ketone-treated trypsin digestion of the *S*-alkylated BmP09. The Met residue labeled with an *asterisk* represents an oxidative modification.

```
BmP09          DNGYLLNKYTGCKIWCVIN--NESCNSECKLRR--GNYGYCYFW---KLACYCEGAPKS-ELWAYETNKCNGKM*   100%
BmK AS-1       DNGYLLNKYTGCKIWCVIN--NESCNSECKLRR--GNYGYCYFW---KLACYCEGAPKS-ELWAYETNKCNGKM    99.5%
Neurotoxin 2   KEGYLVNKSTGCKYGCLKLGENEGCDKECKAKNQGGSYGYCY-----AFACWCEGLPESTPTYPLPNKSCS---    47.1%
Neurotoxin 1   KEGYLVKKSDGCKYDCFWLGKNEHCDTECKAKNQGGSYGYCY-----AFACWCEGLPESTPTYPLPNKSC----    44.1%
BmK I          VRDAYIAKPHNCVYECARN---EYCNDLCTKNG--AKSGYCQWVGKYGNGCWCIELPDNVPIRVPG--KCH---    30.4%
```

FIG. 3. **Sequences alignment of BmP09 with other long chain scorpion toxins.** The sequences of BmK AS-1 (23), neurotoxin 1 (47), neurotoxin 2 (47), and BmK I (48) were obtained from GenBank™ with accession numbers AF079061, AF338454, AF338453, and AF057554. Sequences alignments have been performed according to their cysteine residues, and gaps are presented as *dashes*. Here the *M** represents the sulfoxide methionine.

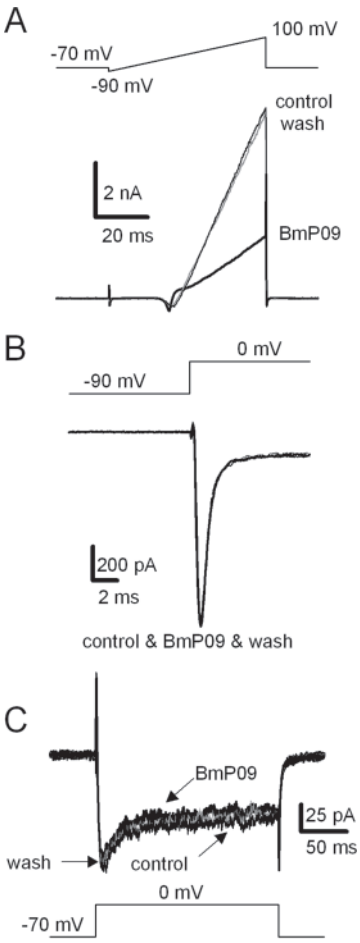


FIG. 4. **Effects of the scorpion toxin BmP09 on $K^+$, $Na^+$, and $Ca^{2+}$ currents in MACCS.** *A*, whole-cell currents were elicited by a 60-ms voltage ramp from −90 mV to +100 mV in the normal extracellular bath solution. The 100 nM BmP09 reduced the outward $K^+$ current around 67% in this cell. *B*, fast inward $Na^+$ currents were activated by a voltage step to 0 mV, after a prepulse to −90 mV to remove inactivation, in the bath solution with 20 mM TEA and 160 mM $Cs^+$ internal solution. A trace obtained at 100 nM BmP09 is nearly the same as in control ($n = 6$). *C*, $Ba^{2+}$ currents were elicited at 0 mV from a holding potential of −70 mV in 160 mM TEA-Cl and 5 mM $BaCl_2$ bath solution. The pipette was backfilled with 160 mM $Cs^+$ solution. At 100 nM, BmP09 results in negligible effects on the inward $Ba^{2+}$ current ($n = 5$).

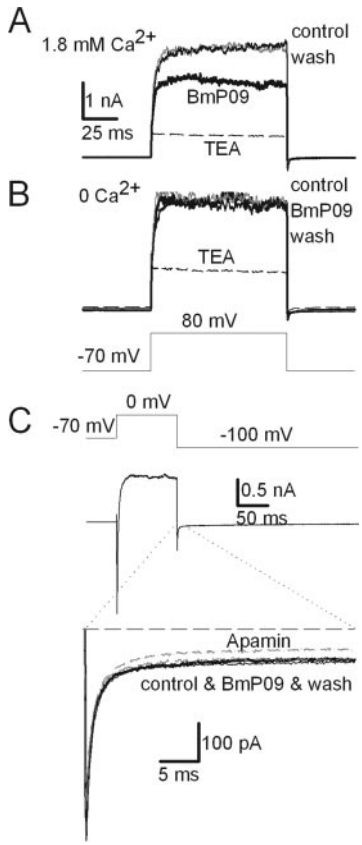


FIG. 5. **BmP09 has no effect on $Ca^{2+}$-independent but voltage-dependent $K^+$ currents, and BmP09 has little effect on SK currents.** *A*, in the 1.8 mM $Ca^{2+}$ bath, the BmP09 partially reduced the $K^+$ current ($n = 10$), in which a $Ca^{2+}$-dependent component should be involved. *B*, in $Ca^{2+}$-free bath solution, the traces of $K^+$ currents, activated by a voltage protocol indicated at the *bottom*, show that BmP09 has no effect on the $K^+$ current ($n = 10$). In both cases, 20 mM TEA was applied in all experiments to obtain net $K^+$ currents. This means that the toxin BmP09 is exclusively sensitive to $Ca^{2+}$-dependent $K^+$ currents. *C*, in the 1.8 mM $Ca^{2+}$ bath solution, SK currents were activated at −100 mV by the $Ca^{2+}$ influx during the 100-ms prepulse to 0 mV from the holding potential −70 mV. A voltage protocol is shown at the *top panel*. At the *bottom panel*, 200 nM apamin was applied to show SK currents in all the patches, and currents in the patch were all in the same level for 0, 100, and 0 nM BmP09 solutions ($n = 15$), which suggested that BmP09 had no effect on SK currents.

channels exist, and the L-type calcium channel is clustered with the BK channels (33). There were three possibilities for the inhibition of BmP09 on outward $K^+$ currents. The first possibility was directly blocking on $Ca^{2+}$-activated $K^+$ currents; the second possibility was directly blocking $K_V{}^+$ channels; and the third possibility was indirectly blocking on the $Ca^{2+}$ channels. Therefore, we intended to verify whether BmP09 blocked voltage-gated calcium channels first. In Fig. 4*C*, $Ca^{2+}$ currents were elicited by 200 ms of depolarization from a holding potential −70 mV to 0 mV. Three traces of $Ca^{2+}$ currents are nearly at the same level for 0, 100, and 0 nM BmP09, which suggests that BmP09 has negligible effects on the inward $Ca^{2+}$ currents. This result also hinted that the BmP09 blocked $K_V{}^+$/BK channels.

*Selectivity of BmP09 among $K^+$ Channels*—$K^+$-selective channels with a tremendous diversity are found in probably all the cells. $K^+$ channels, when they are open, set the resting potential, keep fast action potential short, etc. (34). However, we often do not know which types are present in cells, *e.g.* in MACCs. As we know, there are at least two types of $K_V$ channels, *i.e.* a delayed-rectified channel and an A-type transient channel, and two types of $Ca^{2+}$-dependent $K^+$ channels ($K_{Ca}$) in MACCs, *i.e.* a small conductance $Ca^{2+}$-dependent $K^+$ channel (SK) and a BK channel. It is hard to distinguish their individual types in MACCs, but it is easy to separate $K_V$ and $K_{Ca}$ channels by applications with alternating calcium concentration in the bath solution. In the Fig. 5, *A* and *B*, all traces were activated by 100 ms of depolarization to +80 mV from a holding potential of −70 mV, which was designed to avoid the calcium influx induced by the opening of calcium channels at ~0 mV. In Fig. 5*A*, 100 nM BmP09 obviously blocked the "$K_V$" currents within the normal bath solution, *i.e.* 1.8 mM $Ca^{2+}$ in the normal saline. But as applied with $Ca^{2+}$-free normal saline at the above patch, we found that 100 nM BmP09 had no effect on the remaining currents as shown in Fig. 5*B*. Now we think that traces in Fig. 5*B* present $K_V$ currents only. This also means that the protocol as indicated in Fig. 5*B* cannot completely avoid calcium influx into MACCs for an unknown reason. In all experiments, 20 mM TEA in Fig. 5, *A* and *B,* was applied extracellularly for subtracting leak currents.

Small conductance calcium-activated $K^+$ channels (SK channels) play an important role in modulating excitability in MACCs. SK channels are voltage-independent and activated by submicromolar concentrations of intracellular calcium (35).

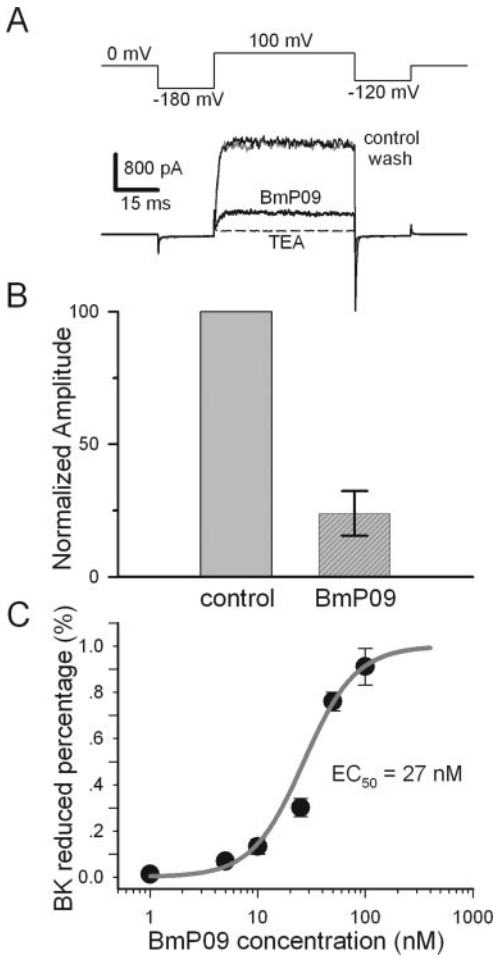


FIG. 6. **BmP09 blocks currents of mSlo1 $\alpha$-subunit expressed in *Xenopus* oocytes.** *A*, traces show the BK currents from an outside-out patch from a *Xenopus* oocyte injected with cRNA encoding mouse Slo1 $\alpha$-subunit. Channels were activated by a voltage step to +100 mV, after a prepulse to −180 mV, in the presence of 10 $\mu$M $Ca^{2+}$. A voltage protocol is shown at the *top panel*. BK currents encoded with mSlo1 were remarkably reduced by 100 nM BmP09. *B*, on an average, 100 nM BmP09 reduced BK currents by 76.1 ± 8.5% ($p < 0.01$, $n = 20$, Student's *t* test). 20 mM TEA was applied before applications of the toxin BmP09 for subtracting leak or native currents. *C*, the dose-response curve of BmP09 blocking BK currents was fitted by the Hill equation (see "Experimental Procedures"). The $EC_{50}$ value is 27 nM, and the Hill coefficient is 1.8 ($n = 5$).

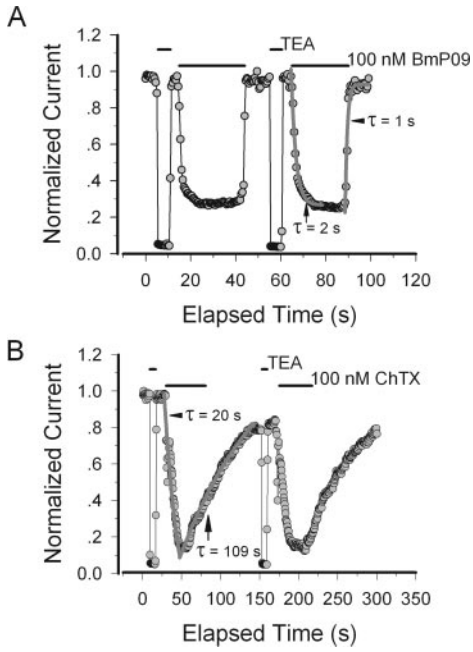


FIG. 7. **The time course of BmP09 blocking BK currents.** *A*, normalized peak current amplitudes from patches shown above are plotted as a function of elapsed time. The patch was perfused with 20 mM TEA and 100 nM BmP09 as indicated by the *horizontal bars*, respectively. Fits to the onset and offset time courses of BmP09-BK give $\tau_{on}$ = 2 s and $\tau_{off}$ = 1 s, respectively. *B*, depolarizations were applied every 500 ms by the protocol indicated in Fig. 6*A*, and as a comparison, the normalized results for 100 nM ChTX are plotted. Fits to the onset and offset time courses of ChTX/BK give $\tau_{on}$ = 20 s and $\tau_{off}$ = 109 s, respectively.

Based on the results shown in Fig. 4 and Fig. 5, *A* and *B*, we know that currents inhibited by BmP09 were $K_{Ca}$ channels. Now we need to identify which channel of $K_{Ca}$, *i.e.* SK or BK, was blocked by the BmP09. In Fig. 5*C*, SK currents were activated by a test pulse to −100 mV after the 100-ms prepulse to 0 mV to upload calcium ions into the cytosolic membrane. In each patch, 200 nM apamin was used to identify the toxin-sensitive components. It is clear that the BmP09 has little effect on the SK currents based on traces shown in the *inset* of Fig. 5*C*. To investigate the detailed blocking effects on BK currents by the BmP09, we adopted *Xenopus* oocytes as an expression system instead of MACCs. In Fig. 6*A*, currents from an outside-out macropatch with 10 $\mu$M $Ca^{2+}$ in the pipette were elicited by a voltage protocol indicated at the *top panel*. In each patch, 20 mM TEA was applied extracellularly to obtain remaining leak currents. By subtracting leak currents, we found that 100 nM BmP09 blocked ~80% (Fig. 6*A*). On average, BK currents were reduced by 76.1 ± 8.5%, with applying 100 nM BmP09 (Fig. 6*B*). The $EC_{50}$ of BmP09 on $BK_{Ca}$ channels was assessed to be 27 nM with a Hill coefficient of $n = 1.8$, according to the dose-response curve fitting (Fig. 6*C*). BmP09 also blocked the inactivating currents of mSlo1/$\beta_2$ coexpressed in *Xenopus* oocytes with over 100 nM $EC_{50}$ (data not shown).

In comparison with the scorpion toxin ChTX, an antagonist of BK channels, the time course of BmP09 blocking BK channels is as indicated in Fig. 7. For BmP09 (Fig. 7*A*), both the onset and offset of blockings are very rapid with a complete recovery. The blocking behavior of BmP09 on BK channels is similar to the TEA-blocking $K^+$ channels. Correspondingly, the time course of 100 nM ChTX (Fig. 7*B*) shows a much slower onset and offset on BK currents with only 80% recovery.

Single channel recordings (Fig. 8), in an outside-out patch with 10 $\mu$M $Ca^{2+}$ in the pipette, were derived from BK channels encoded with the mSlo1 $\alpha$-subunit expressed in *Xenopus* oocytes. Currents were activated every 3 s by depolarizations to 40 mV from a holding potential of −140 mV for 500 ms. Fig. 8*A* shows that the representative sweeps and the ensemble average traces of 20 continuous sweeps in the absence or presence of BmP09, respectively. The corresponding amplitude histograms in Fig. 8*B* are shown below the traces in Fig. 8*A*. Statistical analysis revealed that BmP09 had no effect on single BK channel conductance (~250 pS under symmetrical 160 mM $K^+$ solutions) but reduced the probability of being open or increased the close time of the single BK channel. The total open time of the single BK channel was decreased to almost 30% over the control during applications of 100 nM BmP09. These values were consistent to those of macroscopic BK currents.

*Molecular Modeling of BmP09*—As shown in Fig. 9*A*, the structure of the BmP09 model has the common characteristics of $\alpha$-type toxin. It contains one $\alpha$-helix (residues 22–29), and a three-strand anti-parallel $\beta$-sheet (residues 2–4, 34–37, and 44–47). The $\alpha$-helix is connected to the middle strand of the $\beta$-sheet by a pair of disulfide bonds involving Cys-23 to Cys-44 and Cys-27 to Cys-46. The longer outer strand of the $\beta$-sheet is linked to the long loop prior to the $\alpha$-helix by a disulfide bond

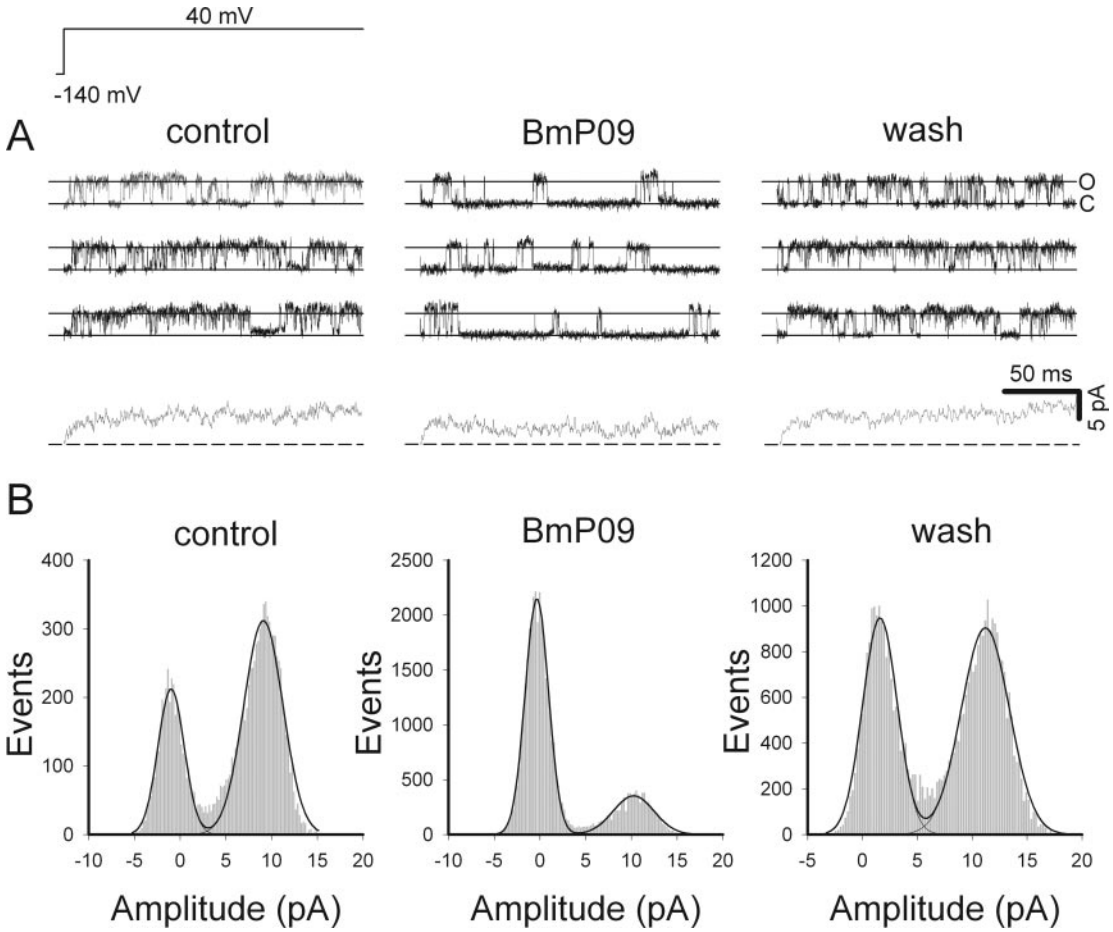


FIG. 8. **Effects of the toxin BmP09 on single BK channels expressed in *Xenopus* oocytes.** *A*, traces in the *middle panel* show single-channel openings of BK channels in an outside-out patch. The cytosolic side of membrane was faced with 10 $\mu$M $Ca^{2+}$. Channels were activated, by voltage steps from −140 mV to +40 mV for 0.5 s, before, during, and after the application of 100 nM BmP09. Ensemble average currents from 20 continuous sweeps are shown below the traces. *B*, the corresponding amplitude histograms show that the average amplitudes of currents, at 40 mV, are 10.1, 10.6, or 9.6 pA, and the probabilities of being open are 69, 22, or 57%, respectively.

between Cys-16 and Cys-37. The fourth disulfide bond between Cys-12 and Cys-62 limits the flexibility of the C terminus. There is an additional shorter two-strand anti-parallel $\beta$-sheet formed by residues 6–7 and residues 12–13 of BmP09, compared with neurotoxin 2.

The surface electrostatic charge distribution of BmP09 is shown in Fig. 9*B*. It contains a dense positively charged region mainly composed of the basic residues Lys-13, Lys-41, and Lys-65. The Lys-41 is located at the loop between the middle strand and outer strand of the $\beta$-sheet; the Lys-65 is located at the C terminus, and the Lys-13 is partially buried. The specificity of scorpion toxin for the various potassium channels has been extensively investigated. The results revealed that binding of the peptide is governed by electrostatic interactions between negatively charged residues in the channel and positively charged residues in the peptide (36, 37). The surface electrostatic distribution shown in Fig. 9*B* indicated that BmP09 preferred association with the entryway of the BK channel by using its positive patch around the side chains of Lys-13, Lys-41, and Lys-65.

The structure of the BmP09-BK channel cluster with the favorable electrostatic energy was further refined, and the optimized structure of BmP09-BK channel complex is shown in Fig. 9*E*. The principal interactions between the toxin BmP09 and the BK channel derived from the refined complex structure were analyzed using the LIGPLOT program (38), and the results are summarized in Table II. Four hydrogen bonds and three hydrophobic contacts existed in the refined complex. Therefore, the interface between the BmP09 and the BK channel is large and involves about 7 residues of BmP09 and 12 residues of the BK channel, respectively.

## DISCUSSION

In the present study, we described the structure and function of the novel scorpion toxin BmP09. We found the following. 1) The amino acid sequence of BmP09 was identical to the BmK AS-1 except for a sulfoxide Met-66 residue at the last C terminus in BmP09. 2) In contrast to BmK AS-1, 100 nM BmP09 selectively blocked BK channels with no effect on $Na^+$ channels based on the results from chromaffin cells. 3) BmP09 reduced the open probability of the reconstituted BK channels encoded with mSlo1 but did not alter the single-channel conductance. 4) A mechanism for BmP09 blocking the mSlo1 channels was proposed by simulating the ligand/channel binding, based on the molecular structures of BmP09 and mSlo1.

*The Features of BmP09 in Blocking BK Channels*—In this study, we have described the purification, characterization, and electrophysiological behavior of BmP09. The sequence of BmP09 is almost identical to that of the known toxin BmK AS-1, with the only difference being an oxidative modification at the C terminus (23, 39). Met-66 with a sulfoxide group makes BmP09 a dramatically different function compared with BmK AS-1. BmK AS-1 blocks the $Na^+$ channel with no effect on $K^+$ channels, whereas BmP09 shows completely opposite results. Upon probing the targets of BmP09 toxin on chromaffin cells, we found that 100 nM BmP09 inhibited BK currents

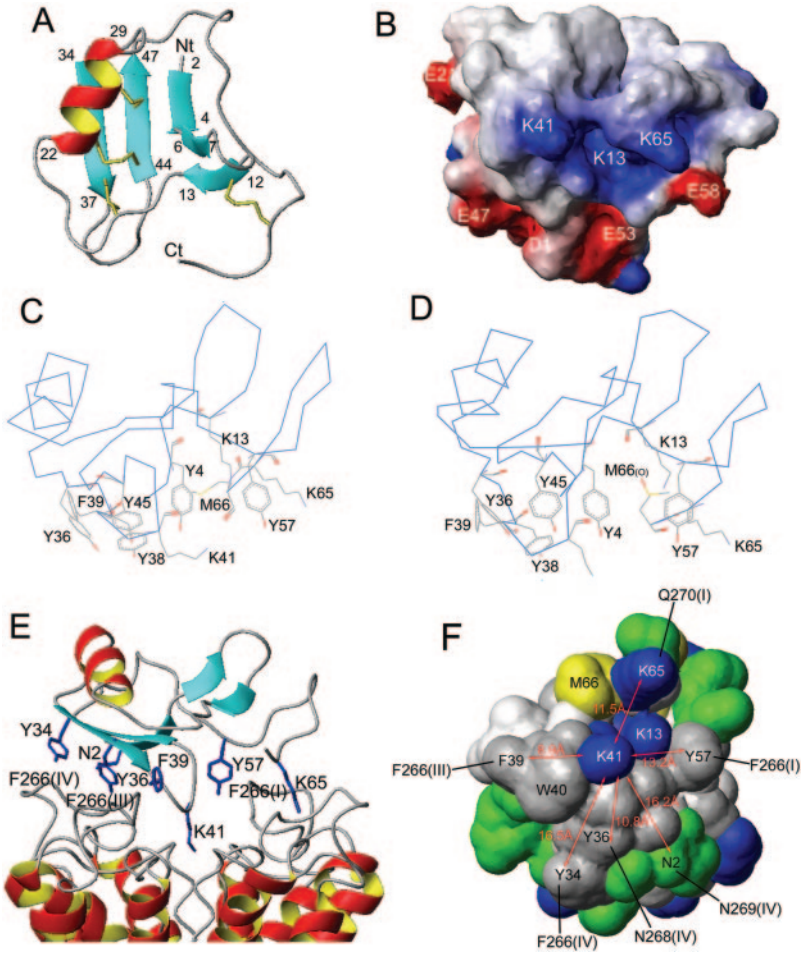


FIG. 9. *A*, MOLMOL representation of the structure of BmP09 model. *Nt* and *Ct* indicate the N terminus and C terminus, respectively. Three disulfide bridges are shown as neons (*yellow*). *B*, electrostatic potential surfaces of BmP09 is calculated by MOLMOL program. Positively charged residues are shown in *blue* and negatively charged residues are shown in *red*, respectively. *C* and *D*, three-dimensional structures of the toxin BmK AS-1 (*C*) and the toxin BmP09 (*D*); residues Tyr-4, Lys-13, Tyr-36, Tyr-38, Phe-39, Lys-41, Tyr-45, Tyr-57, Lys-65, and Met-66 are labeled and their side chains are shown, whereas the other residues are indicated with $\alpha$-carbon atoms shown in *blue*. *E*, the front view of the BmP09-Kca1.1 channel complex generated by MOLMOL. The residues Asn-2, Tyr-34, Tyr-36, Phe-39, Lys-41, Tyr-57, and Lys-65, which have formed hydrogen bonds and hydrophobic contacts with the residues of the channel, are marked. *F*, interaction interface of BmP09 with BK channel. The key interactions pairs are indicated with *black lines*, whereas the interactions between Lys-41 of BmP09 and Tyr-290 (I–IV) of the BK channel are not shown for clearer views. *Blue*, *yellow*, *green*, *white*, and *gray* surfaces represent basic, sulfur-containing, polar, nonpolar, and aromatic residues, respectively. The *red lines* highlight the distance between the key residues and central Lys-41 on the interface of BmP09.

TABLE II
*Observed interactions between the BmP09 scorpion toxin and the BK channel in the BmP09-BK channel complex*

| Observed hydrogen bonds between BmP09 and BK channel | | | | |
|---|---|---|---|---|
| Scorpion toxin BmP09 | | BK channel | | |
| Residue | Atom | Residue[a] | Atom | Distance |
| | | | | Å |
| Asn-2 | O-$\delta$1 | Asn-269(IV) | N-$\delta$2 | 2.96 |
| Tyr-36 | OH | Asn-268(IV) | O-$\delta$1 | 2.84 |
| Lys-41 | N-$\zeta$ | Tyr-290(I) | O | 3.01 |
| Lys-41 | N-$\zeta$ | Tyr-290(II) | O | 2.94 |
| Lys-41 | N-$\zeta$ | Tyr-290(III) | O | 3.00 |
| Lys-41 | N-$\zeta$ | Tyr-290(IV) | O | 3.08 |
| Tyr-57 | OH | Phe-266(I) | O | 2.88 |
| Tyr-57 | OH | Asn-268(I) | O-$\delta$1 | 3.03 |
| Tyr-57 | OH | Lys-296(I) | N-$\zeta$ | 2.91 |
| Lys-65 | N-$\zeta$ | Gln-270(I) | O-$\epsilon$1 | 2.83 |

| Observed hydrophobic contacts between BmP09 and BK channel | |
|---|---|
| Scorpion toxin BmP09 | BK channel |
| Tyr-34 | Phe-266(IV) |
| Phe-39 | Phe-266(III) |
| Tyr-57 | Phe-266(I) |

[a] I–IV represent the four chains of the BK channel.

without affecting other voltage-gated $Na^+$, $K^+$, and $Ca^{2+}$ channels in MACCs. This was further confirmed by blocking directly the BK channels expressed with mSlo1 $\alpha$-subunits in *Xenopus* oocytes. It is well known that most of the long chain scorpion toxins are reported as blockers of $Na^+$ channels. One long chain scorpion toxin TsTxK$\beta$ was only found as a blocker of the voltage-gated noninactivating $K^+$ channel (40). To our knowledge, this is the first report regarding a long chain peptide as a specific blocker of BK channels.

Furthermore, the toxin BmP09 exhibited perfect reversibility in blocking BK channels compared with the ChTX. As shown in Fig. 7*A*, both the onset and offset during BmP09 blocking BK channels were very rapid (less than 5 s), and the recovery was complete. In comparison with ChTX, the offset course of 100 nM ChTX was extremely slow (more than 100 s) and incomplete, as shown Fig. 7*B*. The BmP09 blocking BK currents is very similar to the TEA-blocking $K^+$ channels.

On the other hand, BK channels can be formed by $\alpha$-subunit alone or by $\alpha$-subunit bound with up to four $\beta$-subunits. Coexpression with $\alpha$- and $\beta$-subunits, of which the latter are composed of two transmembrane domains with a long extracellular loop, modifies the kinetic behaviors of BK currents encoded with $\alpha$-subunit alone, such as $Ca^{2+}$ sensitivity and pharmacological properties and so on. Typically, it will reduce the sensitivity to scorpion toxins (6). Actually, the *N*-linked glycosylation of $\beta$-subunits excluding $\beta_1$ plays a role in increasing the $EC_{50}$ of toxins on Slo1 alone to more than 20-fold (41). As compared with ChTX or Iberiotoxin, the toxin BmP09 did not show any notable difference on blocking the inactivated currents coexpressed with the mSlo1 $\alpha$- and $\beta_2$-subunits.

*The Difference in the Solution Conformations of BmP09 and BmK AS-1*—As demonstrated above, the scorpion peptides BmP09 and BmK AS-1 possessing high homology in their primary sequences showed remarkable differences in their specificities toward $Na^+$ and $K^+$ channels. These distinctions may be related to their three-dimensional structures. To differentiate the structural features of these two toxins, we generated their three-dimensional structural models by homology model-

ing. As shown in Fig. 9 (*C* and *D*), these two peptides possessed the same global folding and differed clearly in the conformations of their C-terminal segments. For BmK AS-1, the C-terminal residue Met-66 extends to the hydrophobic center of the molecule as a result of its hydrophobicity to form a sulfur-$\pi$ interaction (42), and its carboxylic group forms a salt bridge with the side chain of the basic residue Lys-41. In BmP09, the C-terminal residue Met-66 with a sulfoxide side chain turns back because of its less hydrophobicity, of which the side chain forms a hydrogen bond with the basic side chain of Lys-13 residue. Therefore, the properties of the residue Lys-41 in these two peptides are in obvious conflict. In BmK AS-1, the residue Lys-41 is less basic for the salt bridge and is partly buried in the hydrophobic center, whereas the basic side chain of Lys-41 residue in BmP09 is free and is exposed to the surface of the molecule. These differentiations should be responsible for their distinct behaviors on $Na^+$ and $K^+$ channels.

*The Possible Interaction Mode of BmP09 with BK Channel*—The mechanisms underlying the blockade of voltage-gated $K^+$ channels by $\alpha$-KTx toxins have been intensively explored in the last decade (11, 43–45) by the modeling analysis of the toxin-$K^+$ channel complex generated by docking and dynamic simulations. In order to elucidate the possible interaction mode, the three-dimensional structural model of the BmP09-BK channel complex was generated by docking and dynamic simulations (Fig. 9*E*). In Fig. 9*E*, the positively charged side chain of Lys-41 lies in the center of the peptide/channel interface to form hydrogen bonds with the four backbone carbonyl groups of Tyr-290. In addition, Asn-2, Tyr-36, Tyr-57, and Lys-65 form hydrogen bonds with the residues Asn-269(IV), Asn-268(IV), Lys-296(I), and Gln-270(I) of the BK channel, respectively. Meanwhile, three aromatic interactions were identified as follows: Phe-39 of BmP09 forms favorable aromatic contacts with Phe-266(III) of the BK channel, whereas Tyr-34 and Tyr-57 of BmP09 form aromatic contacts with Phe-266(IV) and Phe-266(I), respectively. Therefore, the interaction mode of BmP09 indicates that the Lys-41 is in the center as a pore blocker, which is surrounded by a network of hydrogen bonds and aromatic $\pi$-$\pi$ interactions between the peptide and the BK channel. On the basis of simulation, Phe-266 plays an important role in stabilizing the binding of the BmP09 and the BK channel. To confirm the interaction between mSlo1 and BmP09, we mutated the residue Phe-266 of mSlo1 to alanine or leucine. Even though the currents of "F266A/F266L" elucidated by the same protocol shown in Fig. 6*A* were still blocked by 100 nM BmP09 (Fig. 10*A*), however, the percentage of blockade for F266A and F266L was reduced to less than 20% (Fig. 10*B*).

*Comparison of the Interaction Mode between ChTX-BK Channel and BmP09-BK Channel Complex*—The interaction mode of ChTX peptide with BK channel has been investigated in detail by analysis of the complex model derived from the docking and dynamic simulation (22). To rationalize the difference in the reversibility in blocking BK channels between ChTX toxin and BmP09, a comparison of the interaction modes of ChTX-BK and BmP09-BK channel complexes has been made, and the results are summarized in Table III. For the model of the ChTX-BK complex, the central residue Lys-27 is positioned at the center and its positively charged side chain hydrogen bonds with four backbone carbonyl oxygen atoms of Tyr-290 in the selectivity filter. Besides two salt bridges, two hydrogen bonds as well as three aromatic contacts made favorable contributions to the binding. For the BmP09-BK channel complex, besides basic residue Lys-41, which lies in the center of the peptide/channel interface to form hydrogen bonds with the four backbone carbonyl groups of Tyr-290, four hydrogen bonds and three aromatic contacts

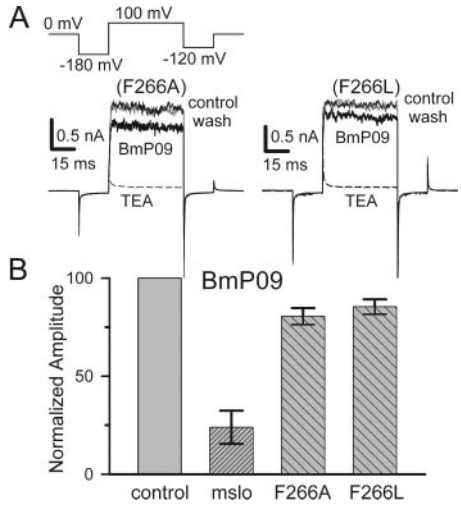


FIG. 10. **F266 stabilizing the conformation of the BmP09-BK channel complex.** *A*, BK currents expressed with cRNA encoding F266L/F266A were activated by the protocol as for Fig. 6*A*, in the presence of 10 $\mu$M $Ca^{2+}$. The BK currents of F266L/F266A were slightly reduced by 100 nM BmP09. *B*, on average, the 100 nM BmP09 only reduced the currents of F266A (*left*) and F266L (*right*) by 19.5 ± 4.2% ($n$ = 14) and 15 ± 3.8% ($n$ = 14), respectively ($p < 0.01$, Student's $t$ test). 20 mM TEA was applied before applications of the toxin BmP09 for subtracting leak or native currents.

TABLE III
*The comparison of the interaction mode between ChTX/BK and BmP09/BK channel complexes*

| Residues of BmP09 | Distance from central Lys41 residue | Interaction formed with BK channel |
|---|---|---|
| | (Å) | |
| Asr-2 | 16.2 | Hydrogen bond |
| Tyr-34 | 16.5 | $\pi$-$\pi$ interaction |
| Tyr-36 | 10.8 | Hydrogen bond |
| Phe-39 | 8.9 | $\pi$-$\pi$ interaction |
| Tyr-57 | 13.2 | $\pi$-$\pi$ interaction and hydrogen bond |
| Lys-65 | 11.5 | hydrogen bond |
| **Residues of ChTX** | **Distance from central Lys27 residue** | **Interaction formed with BK channel** |
| | (Å) | |
| Ser-10 | 5.6 | Hydrogen bond |
| Trp-14 | 7.7 | $\pi$-$\pi$ interaction |
| Arg-25 | 5.9 | Salt bridge |
| Met-29 | 7.6 | Hydrophobic contact and sulfur-$\pi$ interaction |
| Asn-30 | 9.0 | Hydrogen bond |
| Arg-34 | 6.3 | Salt bridge |
| Tyr-36 | 6.0 | $\pi$-$\pi$ interaction |

constitute the primary interactions. However, the distribution of these hydrogen bonds and aromatic interactions around the central residue in these two complexes is quite different. In the ChTX-BK channel complex most hydrogen bonds, salt bridges, and aromatic interactions lie in the inner part of the interface and close to the central residue (within about 6–7 Å); only Asn-30 is about 9 Å apart from the central residue (Table III). Because ChTX is a globular structure with a spherical surface, those inner hydrogen bonds and aromatic interactions close to the central residue should be buried deeply; only Asn-30 lies at the outer edge of the interface. In contrast, in the BmP09-BK channel complex, most hydrogen bonds and aromatic interactions are apart from the central residue (larger than 9 Å) and located at the outer edge of the interface of the complex as shown in Fig. 9*F*. These facts could well account for the difference in the reversibility in blocking BK channels between the ChTX toxin and BmP09. For the ChTX-BK channel complex, both association and disso-

ciation rates should be slower due to a number of inner and buried hydrogen bonds, salt bridges, and aromatic interactions. In comparison, those of the BmP09-BK channel complex must be quicker because its hydrogen bonds and aromatic interactions are located at the outer edge of the interface and are exposed to the solvents.

On the other hand, the time scale of association and dissociation can be further evaluated on the basis of the $K_d$ data. The time scale of a toxin-receptor reaction is set by a formula $K_d = k_{-1}/k_1$, where $k_1$ is the second-order rate constant for binding ($M^{-1}s^{-1}$); $k_{-1}$ is the first-order rate constant for unbinding ($s^{-1}$), and $K_d$ is the equilibrium dissociation constant (M) of the toxin-receptor complex (46). Meanwhile, the time constant for unbinding $\tau_{unbinding} = 1/k_{-1}$. We now use the above formula to estimate the time scale of unbinding for toxin BmP09. By assuming that $\tau_{unbinding}$ of ChTX-BK complex is set to 200 s and the $K_d = 4$ nM (7), we have $k_1 = 1/(\tau_{unbinding} \times K_d) = 1.25 \times 10^6$ $M^{-1}$ $s^{-1}$. Regarding the toxin BmP09, we assume $k_1 = 1.25 \times 10^7$ $M^{-1}$ $s^{-1}$, because the time scale of BmP09 for binding to BK channels is 10-fold fast than the one of ChTX (Fig. 7). Considering that the $K_d = 27$ nM for BmP09, the unbinding time constant for BmP09 is simply obtained to be about 3 s, which is consistent with the experimental data in this study.

Altogether, BmP09 is the first long chain scorpion peptide as a specific and reversible blocker of BK channels. The structural information derived from the modeling and docking analysis may be helpful in designing specific inhibitors of BK channels.

*Acknowledgments*—We thank Dr. Yong-Hua Ji for the gift of BmK AS-1. We also thank Prof. T. A. Jones of Uppsala University, Sweden, for the software program "O" and Tripos, Inc., for the Sybyl6.3 software package.

REFERENCES

1. Schreiber, M., and Salkoff, L. (1997) *Biophys. J.* **73,** 1355–1363
2. Goudet, C., Chi, C. W., and Tytgat, J. (2002) *Toxicon* **40,** 1239–1258
3. Fan, C. X., Chen, X. K., Zhang, C., Wang, L. X., Duan, K. L., He, L. L., Cao, Y., Liu, S. Y., Zhong, M. N., Ulens, C., Tytgat, J., Chen, J. S., Chi, C. W., and Zhou, Z. (2003) *J. Biol. Chem.* **278,** 12624–12633
4. McManus, O. B., Harris, G. H., Giangiacomo, K. M., Feigenbaum, P., Reuben, J. P., Addy, M. E., Burka, J. F., Kaczorowski, G. J., and Garcia, M. L. (1993) *Biochemistry* **32,** 6128–6133
5. Kaczorowski, G. J., Knaus, H. G., Leonard, R. J., McManus, O. B., and Garcia, M. L. (1996) *J. Bioenerg. Biomembr.* **28,** 255–267
6. Garcia-Valdes, J., Zamudio, F. Z., Toro, L., Possani, L. D., and Possan, L. D. (2001) *FEBS Lett.* **505,** 369–373
7. Xia, X. M., Ding, J. P., and Lingle, C. J. (1999) *J. Neurosci.* **19,** 5255–5264
8. Wallner, M., Meera, P., and Toro, L. (1999) *Proc. Natl. Acad. Sci. U. S. A.* **96,** 4137–4142
9. Meera, P., Wallner, M., and Toro, L. (2000) *Proc. Natl. Acad. Sci. U. S. A.* **97,** 5562–5567
10. Xu, C. Q., Brône, B., Wicher, D., Bozkurt, Ö., Lu, W. Y., Huys, I., Han, Y. H., Tytgat, J., Van Kerkhove, E., and Chi, C. W. (2004) *J. Biol. Chem.* **279,** 34562–34569
11. Rodriguez de la Vega, R. C., and Possani, L. D. (2004) *Toxicon* **43,** 865–875
12. Li, H. M., Wang, D. C., Zeng, Z. H., Jin, L., and Hu, R. Q. (1996) *J. Mol. Biol.* **261,** 415–431
13. Wu, H. M., Wu, G., Huang, X. L., and Jiang, S. K. (1999) *Pure Appl. Chem.* **71,** 1157–1162
14. Zhang, N., Li, M., Chen, X., Wang, Y., Wu, G., Hu, G., and Wu, H. (2004) *Proteins* **55,** 835–845
15. Zhang, N., Chen, X., Li, M., Cao, C., Wang, Y., Wu, G., Hu, G., and Wu, H. (2004) *Biochemistry* **43,** 12469–12476
16. Ji, Y. H., Wang, W. X., Ye, J. G., He, L. L., Li, Y. J., Yan, Y. P., and Zhou, Z. (2003) *J. Neurochem.* **84,** 325–335
17. Neely, A., and Lingle, C. J. (1992) *J. Physiol.* (*Lond.*) **453,** 97–131
18. Ding, J. P., and Lingle, C. J. (2002) *Biophys. J.* **82,** 2448–2465
19. Wu, J. J., He, L. L., Zhou, Z., and Chi, C. W. (2002) *Biochemistry* **41,** 2844–2849
20. Morita, T., Hanaoka, K., Morales, M. M., Montrose-Rafizadeh, C., and Guggino, W. B. (1997) *Am. J. Physiol.* **273,** F615–F624
21. Doyle, D. A., Morais, C. J., Pfuetzner, R. A., Kuo, A., Gulbis, J. M., Cohen, S. L., Chait, B. T., and MacKinnon, R. (1998) *Science* **280,** 69–77
22. Gao, Y. D., and Garcia, M. L. (2003) *Proteins* **52,** 146–154
23. Lan, Z. D., Dai, L., Zhuo, X. L., Feng, J. C., Xu, K., and Chi, C. W. (1999) *Toxicon* **37,** 815–823
24. Cook, W. J., Zell, A., Watt, D. D., and Ealick, S. E. (2002) *Protein Sci.* **11,** 479–486
25. Jones, T. A., Zou, J. Y., Cowan, S. W., and Kjeldgaard, M. (1991) *Acta Crystallogr. Sect. A* **47,** 110–119
26. Vogt, W. (1995) *Free Radic. Biol. Med.* **18,** 93–105
27. Zhou, Z., and Neher, E. (1993) *J. Physiol.* (*Lond.*) **469,** 245–273
28. Zhou, Z., and Misler, S. (1995) *J. Biol. Chem.* **270,** 3498–3505
29. Fenwick, E. M., Marty, A., and Neher, E. (1982) *J. Physiol.* (*Lond.*) **331,** 599–635
30. Elhamdani, A., Zhou, Z., and Artalejo, C. R. (1998) *J. Neurosci.* **18,** 6230–6240
31. Neely, A., and Lingle, C. J. (1992) *J. Physiol.* (*Lond.*) **453,** 133–166
32. Tan, Z. Y., Mao, X., Xiao, H., Zhao, Z. Q., and Ji, Y. H. (2001) *Neurosci. Lett.* **297,** 65–68
33. Prakriya, M., and Lingle, C. J. (1999) *J. Neurophysiol.* **81,** 2267–2278
34. Yellen, G. (2002) *Nature* **419,** 35–42
35. Hirschberg, B., Maylie, J., Adelman, J. P., and Marrion, N. V. (1998) *J. Gen. Physiol.* **111,** 565–581
36. Park, C. S., and Miller, C. (1992) *Biochemistry* **31,** 7749–7755
37. Krezel, A. M., Kasibhatla, C., Hidalgo, P., MacKinnon, R., and Wagner, G. (1995) *Protein Sci.* **4,** 1478–1489
38. Wallace, A. C., Laskowski, R. A., and Thornton, J. M. (1995) *Protein Eng.* **8,** 127–134
39. Ji, Y. H., Li, Y. J., Zhang, J. W., Song, B. L., Yamaki, T., Mochizuki, T., Hoshino, M., and Yanaihara, N. (1999) *Toxicon* **37,** 519–536
40. Rogowski, R. S., Krueger, B. K., Collins, J. H., and Blaustein, M. P. (1994) *Proc. Natl. Acad. Sci. U. S. A.* **91,** 1475–1479
41. Jin, P., Weiger, T. M., and Levitan, I. B. (2002) *J. Biol. Chem.* **277,** 43724–43729
42. Meyer, E. A., Castellano, R. K., and Diederich, F. (2003) *Angew. Chem. Int. Ed. Engl.* **42,** 1210–1250
43. Rodriguez de la Vega, R. C., Merino, E., Becerril, B., and Possani, L. D. (2003) *Trends Pharmacol. Sci.* **24,** 222–227
44. Xu, C. Q., Zhu, S. Y., Chi, C. W., and Tytgat, J. (2003) *Trends Pharmacol. Sci.* **24,** 446–448
45. Mouhat, S., Jouirou, B., Mosbah, A., De Waard, M., and Sabatier, J. M. (2004) *Biochem. J.* **378,** 717–726
46. Hille, B. (2001) *Ion Channels of Excitable Membranes*, 3rd Ed., pp. 505–506, Sinauer Associates, Inc., Sunderland, MA
47. Corona, M., Valdez-Cruz, N. A., Merino, E., Zurita, M., and Possani, L. D. (2001) *Toxicon* **39,** 1893–1898
48. Xiong, Y. M., Ling, M. H., Wang, D. C., and Chi, C. W. (1997) *Toxicon* **35,** 1025–1031